Mutations in *MAP3K7* that alter the activity of the TAK1 signalling complex cause frontometaphyseal dysplasia

Emma M. Wade[1], Philip B. Daniel[1], Zandra A. Jenkins[1], Aideen McInerney-Leo[2], Paul Leo[2], Tim Morgan[1], Marie Claude Addor[3], Lesley C. Adès[4], Debora Bertola[5], Axel Bohring[6], Erin Carter[7], Tae-Joon Cho[8], Hans-Christoph Duba[9], Elaine Fletcher[10], Chong A Kim[5], Deborah Krakow[11], Eva Morava[12], Teresa Neuhann[13], Andrea Superti-Furga[14], Irma Veenstra-Knol[15], Dagmar Wieczorek[16], Louise C. Wilson[17], Raoul C.M. Hennekam[18], Andrew J. Sutherland-Smith[19], Tim M. Strom[20], Andrew O.M. Wilkie[21], Matthew A. Brown[2], Emma L. Duncan[2], David M. Markie[22], Stephen P. Robertson*[1]

Figures

Figure 1

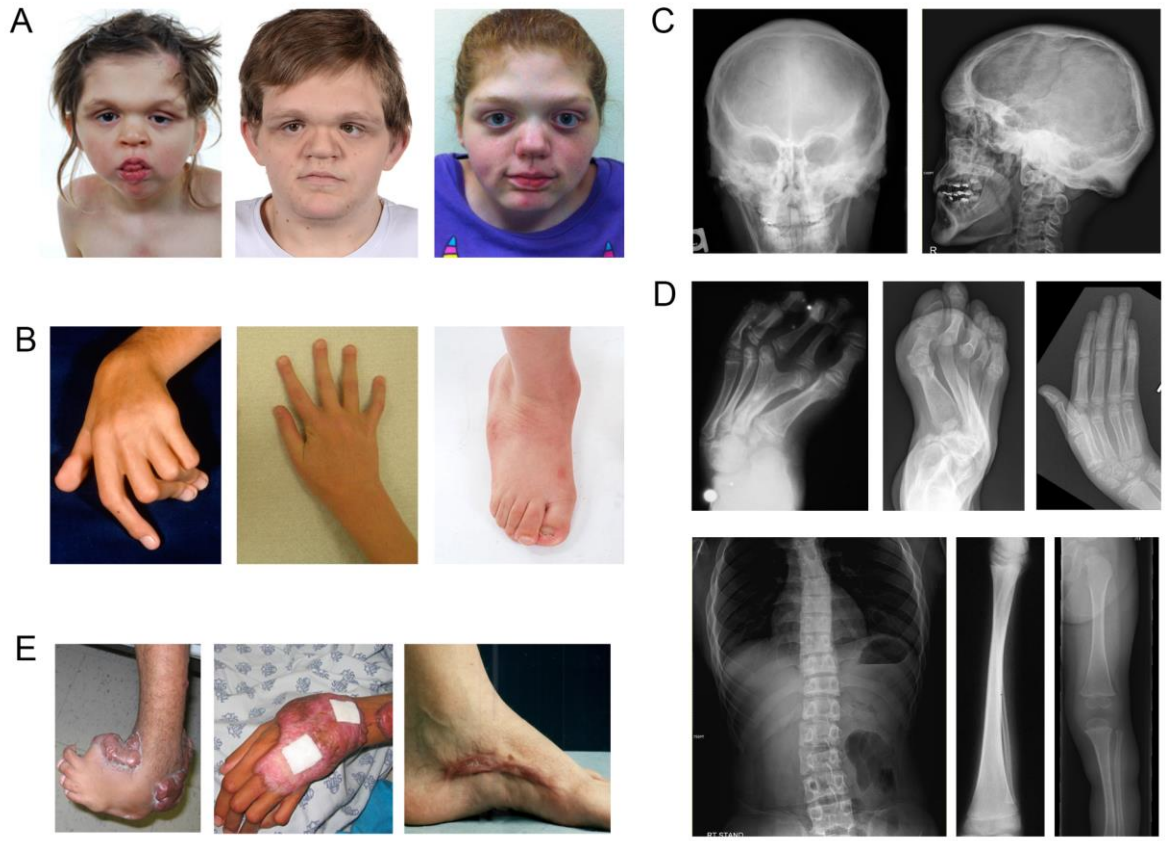

Figure 1: Clinical images of individuals with FMD. (A) Characteristic facial features including supraorbital hyperostosis, downslanting palpebral fissures, hypertelorism, a broad nasal bridge, and a small pointed chin. Panels from left to right show subjects 14, 05, (both TAK1 p.Pro485 Leu) and 17 (TAB2 p.Glu569Lys). (B) Limb abnormalities include contractures of the metacarpophalangeal and interphalangeal joints (subjects 01 and 17), and valgus deformity of the foot (subject 14). Radiological assessment reveals (C) a dense, sclerotic skull especially around the frontal bone and skull base (subjects 09 and 08); (D) undermodelled phalanges, metatarsals and metacarpals (subjects 01, 05, 13) with occasional metacarpal synostosis (subject 01), scoliosis and undermodelled ribs (subject 08), and splaying of the metaphysis of the tibia and femur with bowing (subjects 01 and 02). (E) Keloid scar formation in subjects 11 and 05.

Figure 2

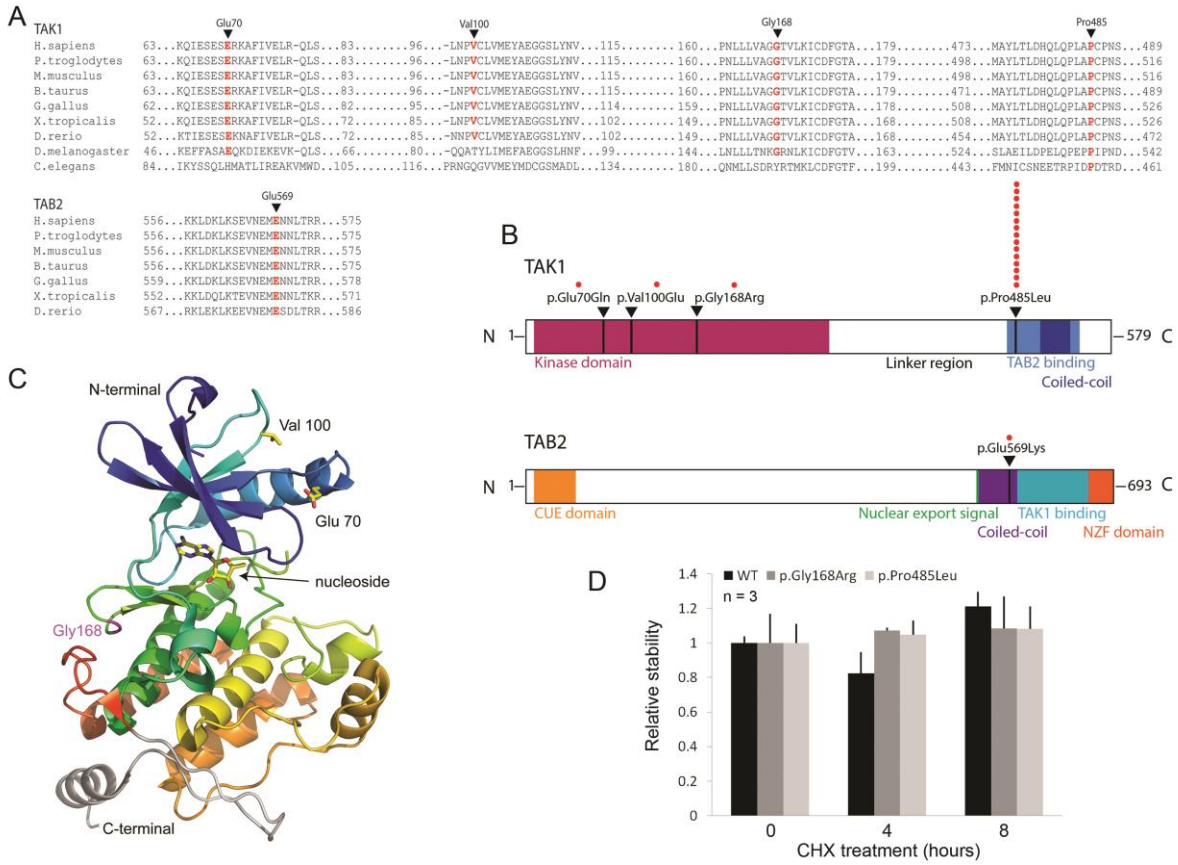

Figure 2: Conservation and structural consequences of substitutions in TAK1 and TAB2. (A) The residues mutated in FMD2 are conserved to *C.elegans* at TAK1^{Pro485}, to *D.melanogaster* at TAK1^{Glu70} and TAK1^{Gly168}, and to zebrafish at TAK1^{Val100} and TAB2^{Glu569}. Sequences were obtained from the Ensembl genome browser and aligned using Clustal Omega, EBI. (B) All five substitutions are found within regions of functional significance; p.Glu70Gln, p.Val100Glu and p.Gly168Arg are located in the middle of the kinase domain (magenta), p.Pro485Leu in located within the TAB2 binding domain on TAK1 (light blue) and p.Gly569Lys is within the coiled-coil domain, of TAB2, which is within the region mapped as critical for TAK1 binding.[27] (C) Crystal structure for the N-terminal 303 amino acids of TAK1; Gly^{168} is located with a tight beta-hairpin turn. Substitution to an arginine at this site has the potential to disrupt the kinase domain. Glu70 is close to a peptide loop which sits over the active site of the TAK1 enzyme, substitution to a glutamine is conservative. Val100 is located in a hydrophobic pocket along with Ile65, Phe74, Arg71 and Leu97, and substitution to a glutamic acid could be destabilising to this region. (D) TAK1$^{p.Pro485Leu}$ or TAK1$^{p.Gly168Arg}$ do not alter the stability of the TAK1 protein when normalised to TAK1^{WT} up to eight hours after cycloheximide treatment of transfected cells. Error bars show standard deviation.

Figure 3

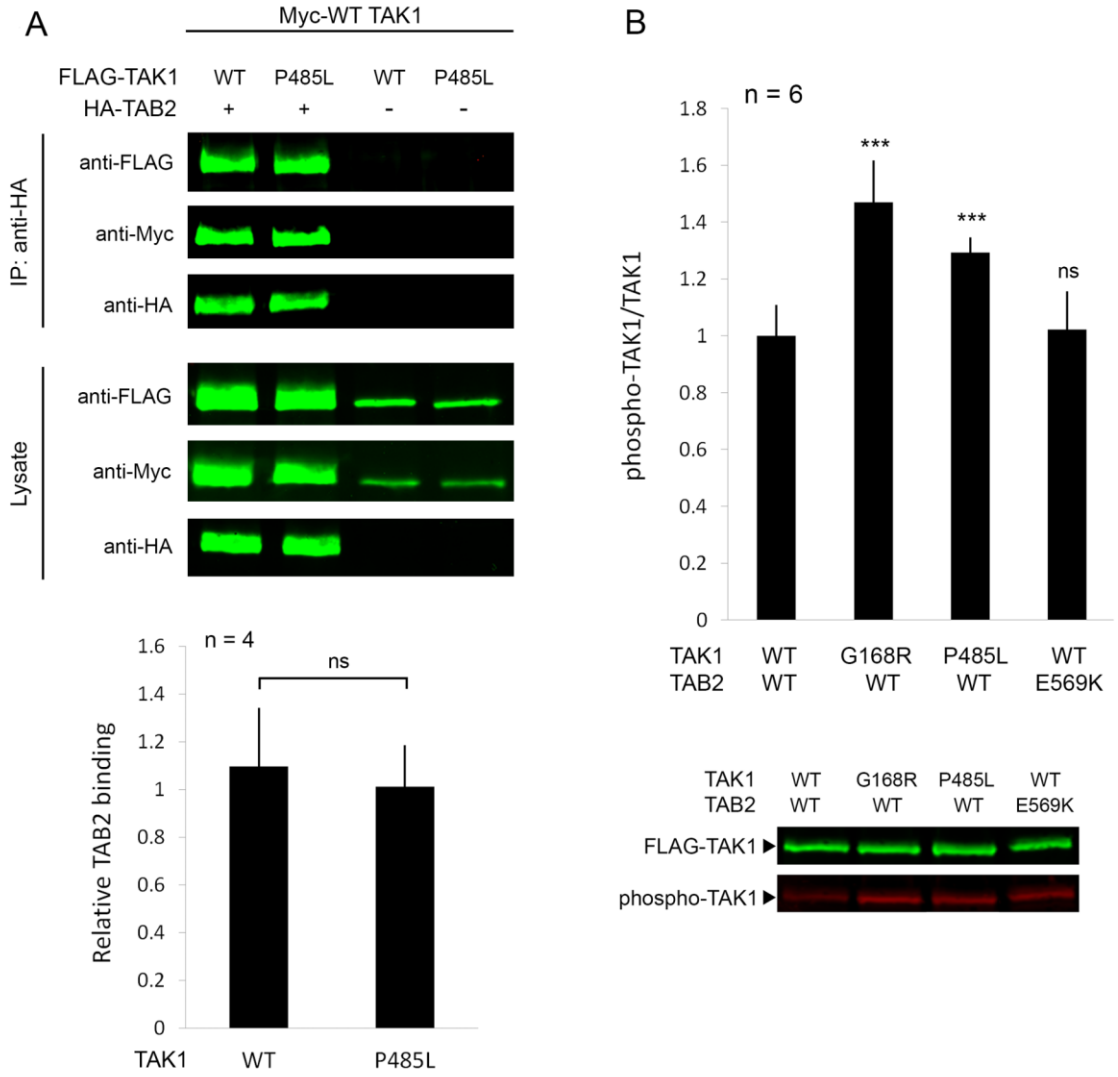

Figure 3: The recurrent TAK1^{Pro485Leu} substitution does not impair TAB2 binding but increases autophosphorylation of TAK1. (A) Competitive co-immunoprecipitation between FLAG-TAK1^{WT} or FLAG-TAK1$^{p.Pro485Leu}$, and HA-TAB2 shows no significant difference between TAK1^{WT} and TAK1$^{p.Pro485Leu}$ in terms of their ability to bind TAB2 in the presence of TAK1^{WT}. (B) When expressed in HEK293FT cells, TAK1$^{p.Pro485Leu}$ and TAK1$^{p.Gly168Arg}$ have significantly increased phosphorylation when expressed with TAB1 and TAB2^{WT} compared to TAK1^{WT}. In contrast, when TAK1^{WT} is expressed with TAB1 and TAB2$^{p.Glu569Lys}$ there is no increased phosphorylation of TAK1. Detection of FLAG was used for the quantification of TAK1. Error bars show standard deviation.

Figure 4

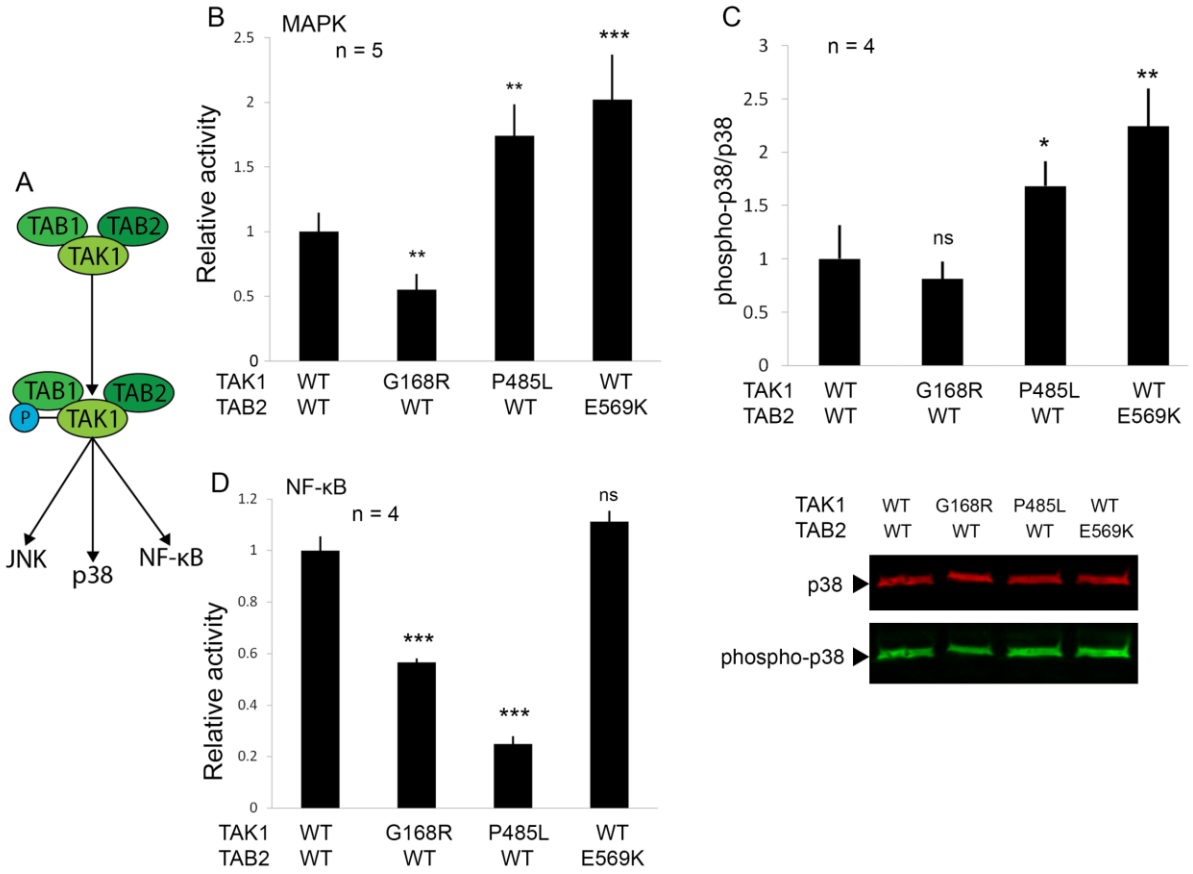

Figure 4: Both MAPK and NF-κB signalling activity are altered by TAK1 and TAB2 substitutions. (A) Activated TAK1 has the ability to activate numerous downstream pathways including those leading to the activation of the kinases JNK and p38, and the pro-inflammatory transcription factor NF-κB. (B) Luciferase reporter for MAPK activity and (C) an immunoblot for phosphorylated-p38, demonstrating that both TAK1$^{p.Pro485Leu}$/TAB2^{WT} and TAK1^{WT}/TAB2$^{p.Glu569Lys}$ combinations are associated with significantly more activated MAPK compared to combinations of WT constructs in HEK293 cells. TAK1$^{p.Gly168Arg}$/TAB2^{WT} is not significantly different from TAK1^{WT}/TAB2^{WT}. (D) The activity of an NF-κB luciferase reporter showed that TAK1$^{p.Pro485Leu}$ and TAK1$^{p.Gly168Arg}$ have significantly reduced NF-κB activity, compared to TAK1^{WT} whereas TAB2$^{p.Glu569Lys}$ was no different to TAK1^{WT} expressed with TAB2^{WT}. Error bars show standard deviation.